2000

Heat Transfer and Pressure Drop Characteristics During of R22 Evaporation In An Oval Micro-fin Tube

M. H. Kim
University of Illinois at Urbana-Champaign

J. S. Shin
Pohang University of Science and Technology

C. W. Bullard
University of Illinois at Urbana-Champaign

HEAT TRANSFER AND PRESSURE DROP CHARACTERISTICS DURING R22 EVAPORATION IN AN OVAL MICRO-FIN TUBE

Man-Hoe Kim[1], Jeong-Seob Shin[2], Clark W. Bullard[3]

[1,3] Department of Mechanical and Industrial Engineering, University of Illinois at Urbana-Champaign
140 MEB, MC-244, 1206 West Green Street, Urbana, IL 61801

[2] Department of Mechanical Engineering, Pohang University of Science and Technology
San 31 Hyoja-Dong, Pohang, Kyungbuk 790-784, Korea

ABSTRACT

An experimental study on R22 evaporating heat transfer in circular and oval micro-fin tubes has been performed. The oval tube was an elliptic tube of axis ratio 1:1.5, which was fabricated from the circular tube with an outer diameter of 9.52 mm and 18° helix angle counterclockwise. The test section was a straight horizontal tube of 0.6 m in length and was heated electrically by a tape heater wound on the tube surface. Heat flux of 12 kW/m^2 was maintained constant and the range of refrigerant quality was 0.2-0.8. The tests were conducted for evaporation at 15°C for 30-60 kg/h mass flow rate (mass flux based on the oval tube: 150-300 kg/m^{2}s) and the installation angles of the oval tube were varied between 0 and 135° in the circumferential direction. The local and average heat transfer and pressure drop characteristics for the oval tube were compared to those for the baseline circular tube. The average heat transfer coefficients for the oval tube were 2-15% higher than that for the round tube and pressure drops for both tubes are similar. The correlations for heat transfer coefficient and friction factor are developed within the rms errors of 4.3% and 10.0%, respectively.

INTRODUCTION

Heat exchangers in air conditioning and heat pump applications have an important effect on system efficiency and physical size, and on environmental impacts. Finned round tube heat exchangers are usually used for the evaporator and condenser for residential air-conditioning systems. The air-side thermal resistance of the heat exchangers dominates the total thermal resistance. To improve the thermal performance of finned tube heat exchangers, it is necessary to reduce air-side thermal resistance. When a round tube is used, heat transfer degradation and large pressure drop are caused by re-circulating flow in the wake, and noise problems may be caused by non-uniform flow at the outlet of heat exchangers. Oval tubes are one option for solving these problems. Therefore, several studies of air-side thermal performance of oval tube heat exchangers have attracted researchers [1-5]. To investigate the overall performance of the oval tube heat exchangers, however, tube-side heat transfer and pressure drop behaviors as well as air-side performance must be considered simultaneously. Several investigators [6-13] performed studies on evaporation in microfin round tubes.

Yasuda et al. [6] developed "THERMOFIN-HEX TUBE", which was 9.52 mm o.d. microfin tube with 18 degree helix angle, to improve the evaporation performance of room air conditioners. They reported R22 evaporation heat transfer coefficient had a maximum at mass flux of 200-250 kg/m^{2}s. Schlager et al. [7] investigated evaporation and condensation heat transfer and pressure drop characteristics in three horizontal 12.7 mm microfin tubes with R22. They found evaporation and condensation heat transfer coefficients in the microfin tubes were 1.6-2.2 and 1.5-2.0 times, respectively, larger than those in the smooth tubes. Kandlikar [8] presented a flow boiling heat transfer correlation for enhanced tubes by modifying his smooth tube correlation, and Christoffersen et al. [9] investigated local evaporation heat transfer and pressure drop characteristics for R22, R134a and R32/R125 (60/40%) in smooth and micro-fin tubes. Kaul et al. [10] conducted study on horizontal evaporation heat transfer performance of R22 and several alternative refrigerants in a fluid heated microfin tube and they developed correlations of heat transfer coefficients for each refrigerant. Chamra et al. [11] presented R22 evaporation heat transfer and pressure drop data for new microfin geometries applied to the inner surface of 15.88 mm o.d. tubes. Kuo et al. [12] reported the effect of heat flux, mass flux and evaporation pressure on the heat transfer coefficients using 9.52 o.d. microfin and plain tubes. Liu [13] performed the study on the evaporating and condensation heat transfer and pressure drop behaviors

of R134a and R22 in a 9.52 mm o.d. axially grooved tube and presented heat transfer coefficient and pressure drop correlations for each refrigerant. Dunwoody and Iqbal[14] investigated single phase laminar heat transfer characteristics in elliptical tubes having different ratios of major and minor axis. They reported that the heat transfer and pressure drop for the elliptic tube are larger than those of a round tube. However, there is no published data in the open literature for refrigerant evaporation in an oval micro-fin tube.

This study investigates local and average heat transfer and pressure drop characteristics during R22 evaporation in a horizontal oval micro-fin tube. The test results are compared to those for a round tube of the same circumferential length. The effect of installation angle on the evaporation characteristics of the oval tube is also reported, and the heat transfer and pressure drop correlations are developed.

EXPERIMENTS

Test apparatus

Figure 1 shows schematic diagram of the test apparatus. It consists of circulation loops for the refrigerant and heat transfer fluids and data acquisition system. The refrigerant circulation loop includes a gear pump, a mass flow meter, a pre-heater, a test section, a stabilizer, a sub-cooling unit and a receiver. The refrigerant is delivered to the test section by the magnetic gear pump. The refrigerant quality at the inlet of the test section is regulated through heat exchange between the refrigerant and the hot water in the pre-heater. Table 1 describes geometrical parameters for the test tubes, compared to those of ACRC [9] and NIST [10]. The test section has an effective length of 600 mm and the oval tube tested was fabricated using 9.52 mm o.d. round micro-fin tube with 18° helix angle counterclockwise. The oval tube is an elliptic tube with axis ratio of 1.5 (major axis: D_m=11.20 mm, minor axis: D_n=7.47 mm), so its cross sectional area is about 10% smaller. A variable power supply was connected to the sheathed heater wound on the tube surface to control the heat flux of the test section. Thermocouples and pressure transducers are inserted in the inlet and outlet of the test tube and a differential pressure sensor is connected between them. The measured saturation temperatures were in good agreement with the temperature calculated based on the measured saturated pressure within ±0.3°C. To measure the tube surface temperatures, twelve thermocouples were attached on the outer surface of the tube at each three locations along the length of the tube, mounted at the top, bottom, right and left of the tube in the circumferential direction. The entire refrigeration circulation loop including the test section was wrapped with 40 mm thick foam insulation to minimize heat transfer between refrigerant and the environment. The pre-test results using water showed that heat balance between heater and water heat transfer was in good agreement within 3%.

The hot and cold water circulation loops to control the state of the refrigerant include a pre-heater and a sub-cooler. Thermocouples were inserted to measure the temperatures at the inlet and outlet of the sub-cooler and pre-heater, and thermopiles were attached to measure the temperature differences between the inlet and outlet of the hot and cold water. Heat transfer rate of the pre-heater was regulated by water flow rate measured using a Micro-motion mass flow meter with an accuracy ±0.2%, which fixed the refrigerant quality at the inlet of the test section. The test data were collected using a hybrid recorder and analyzed in real time with a PC running the data reduction program. All the information about test conditions and test data during the test, were displayed on the monitor and test conditions were changed based on this information.

Test condition and method

The test conditions described in Table 2 are span the range of operating conditions of an evaporator for a residential air conditioning system. The tests are conducted for evaporation at 15° for 30-60 kg/h mass flow rate with R22. The refrigerant flow rate (mass flux of the oval tube: 150-300 kg/m^{2}s) is changed by regulating input power of the magnetic gear pump. Constant heat flux of 12 kW/m^2 based on average inside tube surface area is maintained through all the tests. The quality of the refrigerant entering the test section is controlled through the heat exchange rate in the pre-heater, and the heat flux was maintained modulating the power of the sheathed heater. The installation angles of the oval tube are varied between 0 and 135° in the circumferential direction for investigating the effect of gravitational force on evaporation. Installation angle of 0° designates that the major axis of the oval tube is horizontal, normal to the direction of gravitational force. The test conditions and data to be collected were monitored throughout the test, and the data set of 60-100 were recorded and averaged over 6-10 minutes after test conditions reached the steady state.

Data reduction

The evaporation heat transfer coefficients were calculated as:

$$h = \frac{q_i''}{T_w - T_r} \tag{1}$$

Where q_i'' is heat flux, T_w and T_r are inside wall and refrigerant temperatures, respectively. Heat flux was determined using inside tube wall area, based on the average of root and minimum inner diameters and power input supplied to the heater. T_w was calculated from the measured at outside tube wall temperature using one dimensional conduction equation. Pressure drop data were obtained simultaneously from the differential pressure transducer with 0.17 kPa accuracy and two absolute pressure transducers installed at the inlet and outlet of the test section, and two values were in good agreement. Average heat transfer coefficient and pressure drop data were obtained, respectively, from the average values of the integral of local heat transfer coefficient and pressure drop values, which were fitted over the quality ranges of 0.2-0.8. Refrigerant properties were calculated using REFPROP[15]. Accounting for all instrument errors, uncertainty for the average heat transfer coefficients were 5.9-10.3% [16].

RESULTS AND DISCUSSION

Heat transfer results

Before considering heat transfer behaviors, experimental flow patterns are presented on the Taitel-Dukler map [17] since two-phase heat transfer is strongly dependent of flow pattern. Modified Froude numbers in the figure were calculated using different length scales (D_e) for each installation angle (θ); $D_e=D_n$ for θ=0° and $D_e= D_m \sin\theta$ for 90° and ±45°. Flow patterns for most of test data are in the annular flow regime except for very low quality (x<0.2) and for lower mass flux (m ≤ 45 kg/h) and quality as shown in Figure 2.

Figures 3-5 compare temperature variations along the circumferential direction for the round and oval tubes with 0° and 90° installation angles. The circumferential temperature distribution for 90° installation angle is similar to the round tube and it indicates that flow regime is stratified wavy flow for low mass flow rate (30 kg/h) over the whole quality range. Temperatures of the bottom and right walls are relatively higher than those of the top and left walls since liquid layers are thicker because of gravitation and counterclockwise helix. However, as the refrigerant flow rate increases and flow regime changes to annular flow, the temperature variation along the circumference decreases. On the other hand, for 0° installation angle in which the major axis is horizontal, temperature variation along the circumference is relatively small and temperature difference between the surface and refrigerant is also small compared to 90° installation angle. This may explain the relatively higher heat transfer.

Figure 6 presents local heat transfer behaviors with the refrigerant quality and mass flow rate. The local heat transfer coefficients are increased with refrigerant quality as expected except at low mass flux and low quality region, where flow regime is stratified wavy flow and heat transfer coefficients are relatively constant with quality. The effect of installation angle on the heat transfer coefficient decreases with increasing refrigerant quality and mass flow rate. This behavior may be partly due to the flow regime transition from stratified wavy flow to annular flow and more complete wall wetting and thinning of the liquid film [9].

Figure 7 shows how average heat transfer coefficients vary with mass flux and installation angle. Average heat transfer coefficients for the oval tube are consistently 2-15% higher than that for the round tube for all mass fluxes considered in the study. The heat transfer coefficients had maximum values at the refrigerant flow rate of around 45 kg/h, where mass fluxes of round and oval tubes are 206 and 225 kg/m^{2}s, respectively. This behavior is consistent with the test result for the study of Yasuda et al. [6] who used the same round micro-fin tube.

Table 2 presents heat transfer enhancement factors defined by

$$\eta_h = \frac{h_{oval}}{h_{round}} \tag{2}$$

where h_{oval} and h_{round} are average heat transfer coefficients for the round and oval tubes, respectively and they are fitted using third-order polynomial functions of mass flux, G. For the round tube, η_h is 1.

The heat transfer correlation is obtained using heat transfer enhancement factor (η_h), Boiling number (Bo) and liquid only Reynolds number (Re_{lo}) based on hydraulic diameter (D_h), as defined in Kedzierski and Goncalves [18].

$$Nu = \frac{hD_h}{k_f} = 43.54\eta_h Bo^{\alpha} \mathrm{Re}_{lo}^{\beta} \mathrm{Pr}_f^{0.4} \tag{3}$$

$$\alpha = 0.475 - 0.476x + 0.197x^2, \quad \beta = 0.599 - 0.474x + 0.282x^2 \tag{4}$$

The quadratic exponents in equation (4) have been shown to be very successful for correlating convective boiling with a single expression [10,19]. Figure 8 presents comparison of the present test data and ACRC [9] and NIST R22 data [10], which their tube configurations are similar to the baseline round tube as shown in Table 1, with the present correlation. It predicts well the present test data within rms errors 4.3%, and ACRC and NIST data 17.6 and 9.8%, respectively. The latter studies included a wider range of test conditions, and the ACRC tube geometry had significantly different apex angle (see Table 1).

Pressure drop results

Figures 9-11 show pressure drop results. As shown in Figure 9, local pressure drops for both round and oval tubes increase with quality as expected. However, incremental rate decreases over certain quality and it varies with mass flow rate. For lower mass flow rate (30 and 45 kg/h), incremental rates decrease over vapor quality of 0.65, while for 60 kg/h mass flow rate it decreases over quality of 0.55. As the quality or mass flow rate increases and the liquid layer becomes thinner, the roughness of the liquid-vapor interface decreases and therefore, pressure drop decreases [9]. Figure 10 shows average pressure drop for the oval tube, compared to that of round tube at the same mass flux, and they are similar. However, the average pressure drop in the oval tube at the same mass flow rate is 3-20% greater than that in the round tube, since the cross section area (55.6 mm^2) of the oval tube is smaller than that of the round tube (60.8 mm^2).

Considering that the pressure drop is a characteristic of the friction with the vapor flow [9,13], it can be expressed using friction factor (f), mass flux (G), quality (x), and vapor density (ρ_g):

$$\Delta P = f \frac{\Delta l}{D_h} \frac{(Gx)^2}{2\rho_g} \tag{5}$$

$$f = 0.212 \mathrm{Re}_g^{-0.112} x^{-1.035} \tag{6}$$

Where friction factor f, was correlated to the vapor Reynolds number (Re_g) and quality (x). The friction factor correlation predicts the present and ACRC data [9] within rms errors 10.0% and 15.5 %, respectively.

CONCLUDING REMARKS

Evaporation heat transfer and pressure drop characteristics of R22 in a micro-fin oval tube have been investigated. The average heat transfer coefficients in an oval tube were 2-15% larger than that in the round tube with the same micro-fin and circumference, while pressure drops for both tubes were similar, based on the mass flux. The installation angle of the oval tube did not affect significantly on the evaporation behaviors. The heat transfer enhancement factor for the oval tube was defined based on the round microfin tube, and the quality dependent exponents enabled the single correlation to predict most of two-phase heat transfer coefficients. The correlations for heat transfer coefficient and friction factor were developed within rms errors of 4.3 % and 10.0 %, respectively.

ACKNOWLEDGEMENTS

We are grateful for supporting of this study to Samsung Electronics Co., Ltd. and the 25 member companies of the Air Conditioning and Refrigeration Center (ACRC) at the University of Illinois at Urbana-Champaign. We are also grateful to Dr. Mark A. Kedzierski of NIST for providing the valuable data and comments.

REFERENCES

1. Brauer, H., "Compact heat exchanger, 1964," Chemical and Process Engineering," pp. 451-460.
2. Ota, T. and Nishiyama, H., and Takao, Y., 1984, "Heat transfer and flow around an elliptic cylinder," Int. J. Heat Mass Transfer, Vol. 27, No. 10, pp. 1771-1779.
3. Chen, Y, Fiebig, M., and Mitra, N.K., 1998, "Conjugate heat transfer of a finned oval tube PART A: Flow patterns," Numerical Heat Transfer, Part A, Vol. 33, pp. 371-385.
4. Chen, Y, Fiebig, M., and Mitra, N.K., 1998, "Conjugate heat transfer of a finned oval tube PART B: Heat transfer behaviors," Numerical Heat Transfer, Part A, Vol. 33, pp. 387-401.
5. Y.-H. Choi, S.-T., Kim, and D.-Y. Sohn, , 1998, "Navier-Stokes code development for performance assessment of fin-tube heat exchanger," Ajou University Report 1998A1546, Suwon, Korea.
6. Yasuda, K., Ohizumi, K., Hori, M., and Kawamata, O., 1990, "Development of condensing Thermofin-HEX-C tube," Hitachi Cable Review, No. 9, pp. 247-252.
7. Schlager, L.M., Pate, M.B., and Bergles, A.E., 1990, "Evaporation and condensation heat transfer and pressure drop in horizontal, 12.7-mm microfin tubes with refrigerant 22," Journal of Heat Transfer, Vol. 122, pp. 1041-1047.
8. Kandlikar, S.G., 1991, "A model for correlating flow boiling heat transfer in augmented tubes and compact evaporators," Journal of Heat Transfer, Vol. 113, pp. 966-972.
9. Christoffersen, B.R., Chato, J.C., Wattelet, J.P, and Souza, A.L., 1993, "Heat transfer and flow characteristics of R-22, R-32/R-125 and R-134a in smooth and micro-fin tubes," ACRC Technical Report 47, University of Illinois at Urbana-Champaign.
10. Kaul, M.P., Kedzierski, M.A., and Didion, D.A., 1996, "Horizontal flow boiling of alternative refrigerants within a fluid heated micro-fin tube," Process, Enhanced and Multiphase Heat Transfer: A Fesischrift for A.E. Bergles, Begell House, Inc., New York, pp. 167-173.
11. Chamra, L.M. Webb, R.L., and Randlett, M.R., 1996, "Advanced micro-fin tubes for evaporation," Int. J. Heat Mass Transfer, Vol. 39, No. 9, pp. 1827-1996.
12. Kuo, S.C. and Wang, C.C., 1996, "In-tube evaporation of HCFC-22 in a 9.52 mm micro-fin/smooth tube," Int. J. Heat Mass Transfer, Vol. 39, No. 12, pp. 2559-2569.
13. Liu, X, 1997, "Condensing and evaporating heat transfer and pressure drop characteristics of HFC-134a and HCFC-22," Journal of Heat Transfer, Vol. 119, pp. 158-163.
14. Shah, R. K. and London, A. L., 1978, "Laminar flow forced convection in ducts," Academic Press, pp. 247-252.
15. Huber, M., Gallagher, J., McLinden, M., and Morrison, G., 1996, NIST Thermodynamic Properties of Refrigerants and Refrigerant Mixtures Database - REFPROP, Version 5.1, NIST, U.S.A.
16. Moffat, R.J., 1988, "Describing the uncertainties in experimental results", Experimental thermal and Fluid Science, Vol. 1, pp. 3-17.
17. Taitel, Y. And Dukler, A.E., 1976, "A model for predicting flow regime transitions in horizontal and near horizontal gas-liquid flow," AIChE Journal, Vol. 22, No. 1, pp. 47-55.
18. Kedzierski, M.A. and Goncalves, J.M., 1999, "Horizontal convective condensation of alternative refrigerants within a micro-fin tube," Enhanced Heat Transfer, Vol. 6, pp. 161-178.
19. Kedzierski, M.A. and Kim, M.S., 1998, "Convective boiling and condensation heat transfer with a twisted-tape insert for R12, R22, R152a, R134a, R290, R32/134a, R32/R152a, R290/R134a, R134a/R600a," Thermal Science and Engineering, Vol. 6, No. 1, pp. 113-122.

Table 1 Geometrical parameters for the test tubes

Tube type	Average/ Root diameter (mm)	Major(D_m)/ Minor(D_n) axis (mm)	Bottom/ Mean wall thickness (mm)	Fin height (mm)	Helix/ Apex angle (°)	Number of fins	Hydraulic diameter (mm)	Cross sectional area (mm^2)	Area ratio (A/A_p)
Oval	-	11.2/7.47	0.3/0.36	0.2	18/40	60	5.0	55.6	1.6
Baseline	8.8/8.92	-	0.3/0.36	0.2	18/40	60	5.5	60.8	1.6
ACRC [9]	8.71/8.89	-	0.32/0.41	0.18	18/25	60	5.66	59.6	1.54
NIST [10]	8.8/8.92	-	0.3/0.4	0.2	18/50	60	5.45	60.8	1.6

Table 2 Test conditions

Refrigerant	R22
Evaporating temperature (°C)	15
Mass flow rate (kg/h)	30, 45, 60
Heat flux (kW/m^2)	12
Quality range	0.2-0.8
Installation angle (°)	0, 45, 90, 135 (-45)

Table 3 Heat transfer enhancement factors, η_h

Mass flux (kg/m^2s)	Installation angle (°)			
	0	45	90	-45
150	1.04	1.02	1.05	1.08
225	1.09	1.05	1.07	1.09
300	1.15	1.11	1.10	1.13

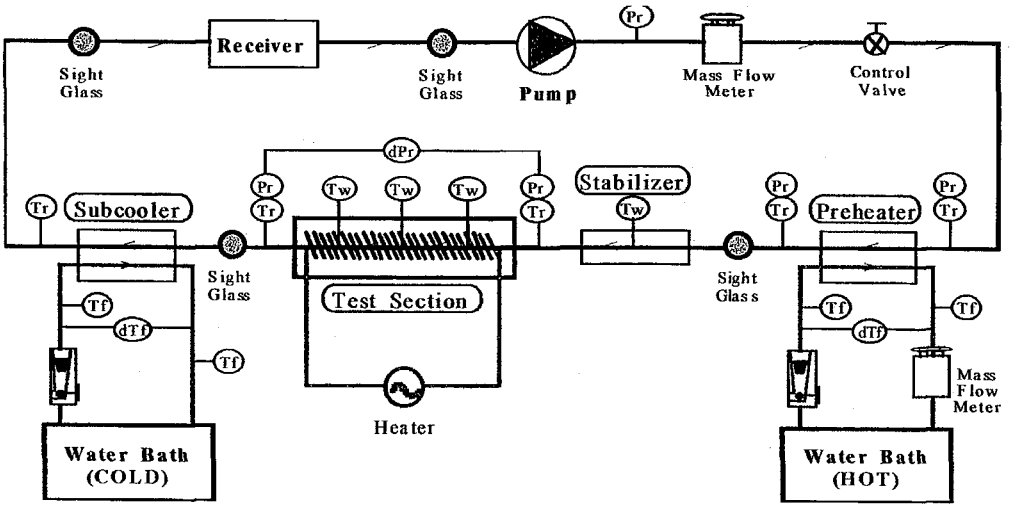

Figure 1. Schematic diagram of test rig

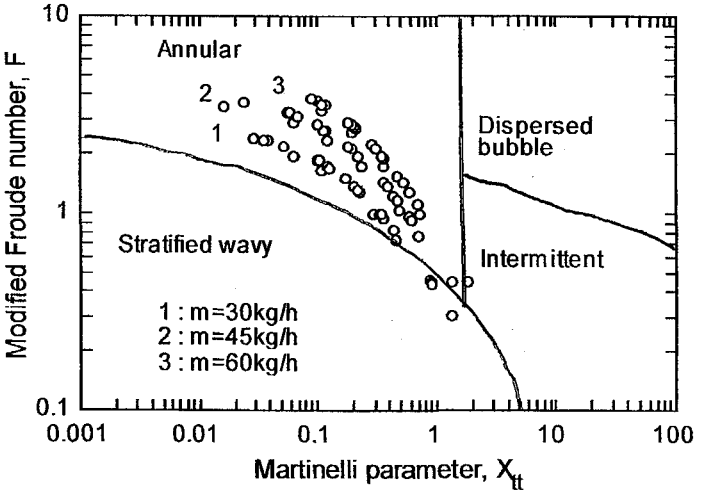

Figure 2. Experimental flow patterns on the Taitel-Dukler map

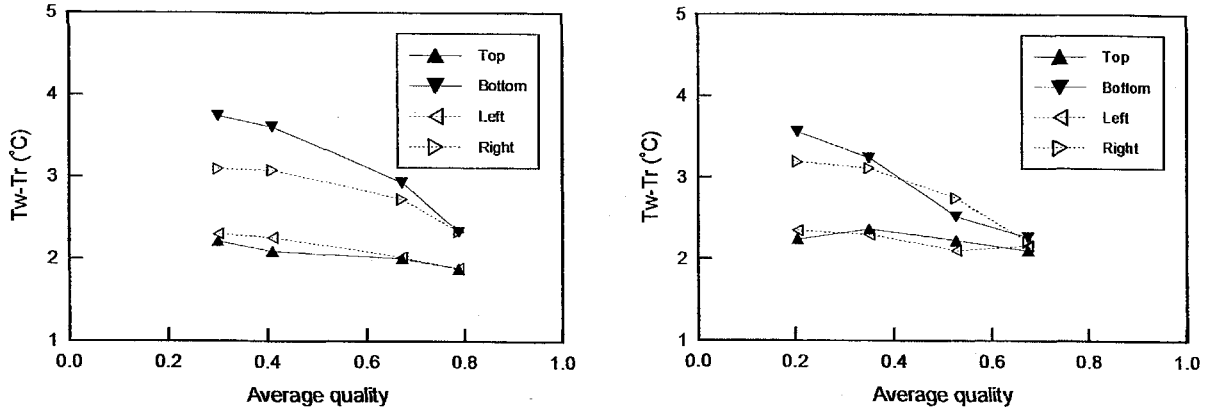

(a) Mass flow rate: 30 kg/h

(b) Mass flow rate: 60 kg/h

Figure 3. Circumferential variations of wall temperatures for the round tube

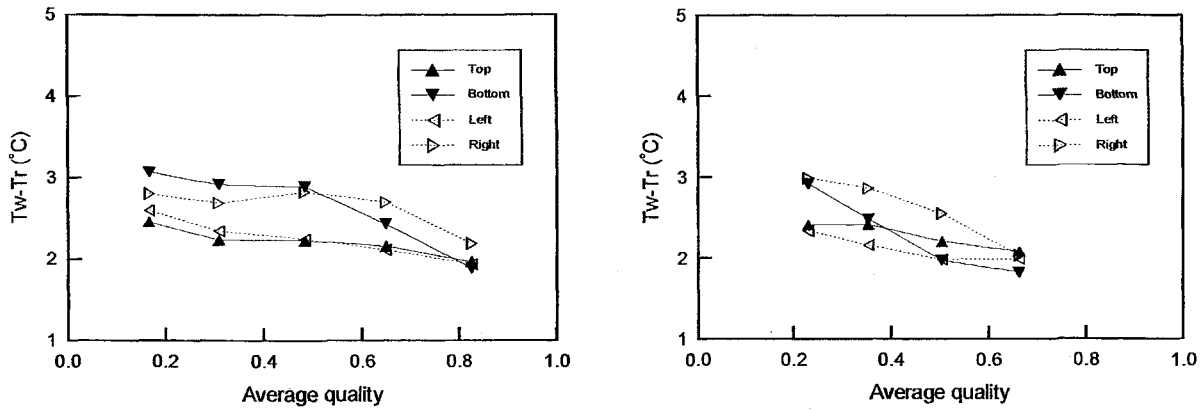

(a) Mass flow rate: 30 kg/h (b) Mass flow rate: 60 kg/h

Figure 4. Circumferential variations of wall temperatures of the oval tube (0° installation angle)

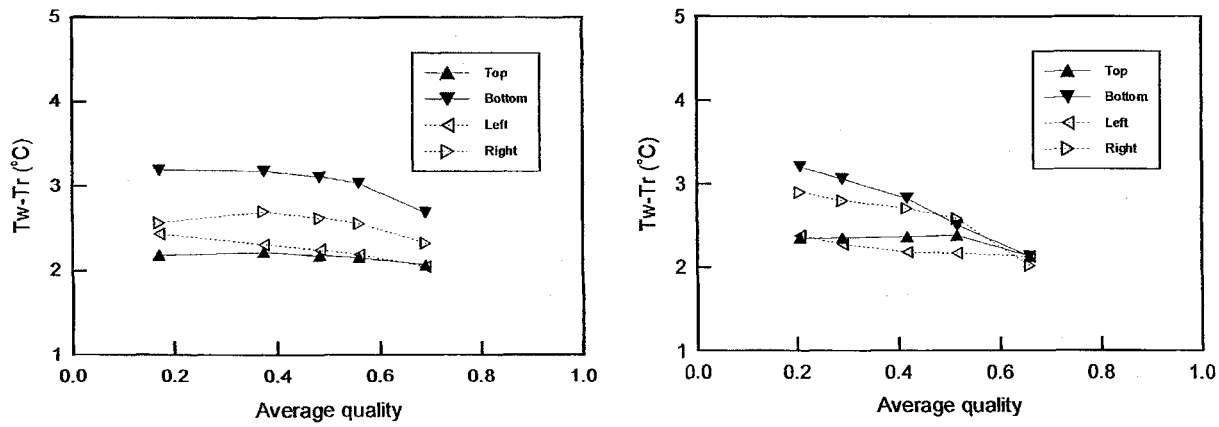

(a) Mass flow rate: 30 kg/h (b) Mass flow rate: 60 kg/h

Figure 5. Circumferential variations of wall temperatures of the oval tube (90° installation angle)

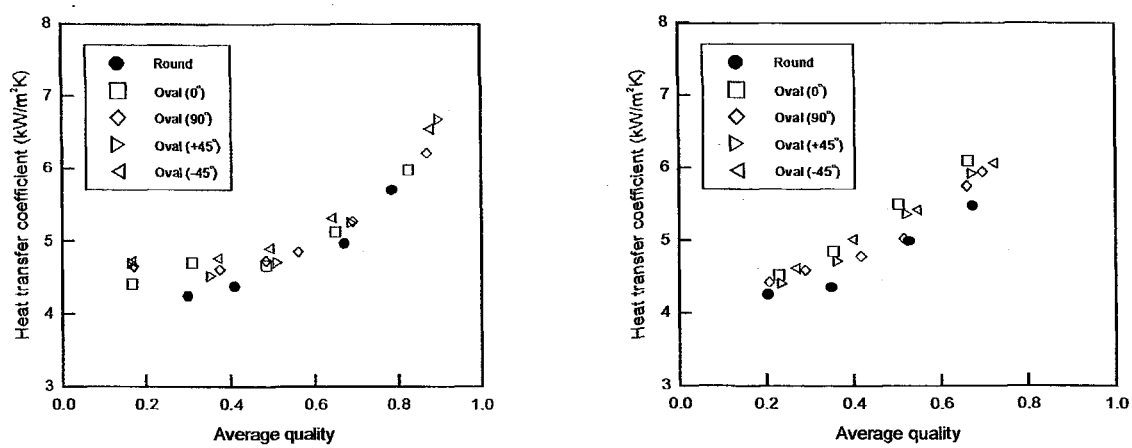

(a) Mass flow rate: 30 kg/h (b) Mass flow rate: 60 kg/h

Figure 6. Local heat transfer coefficients

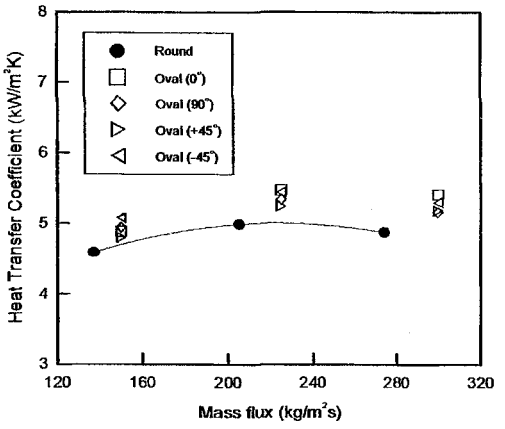

Figure 7. Average heat transfer coefficients with variation of mass flux

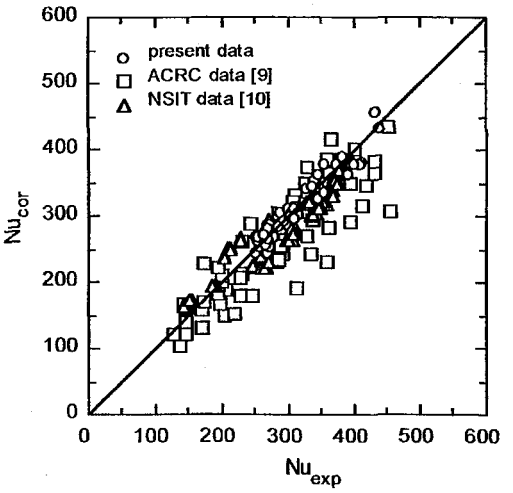

Figure 8. Comparison of experimental data and Nu correlation

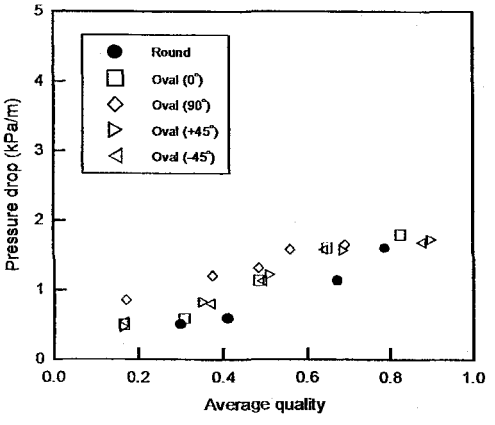

(a) Mass flow rate: 30 kg/h

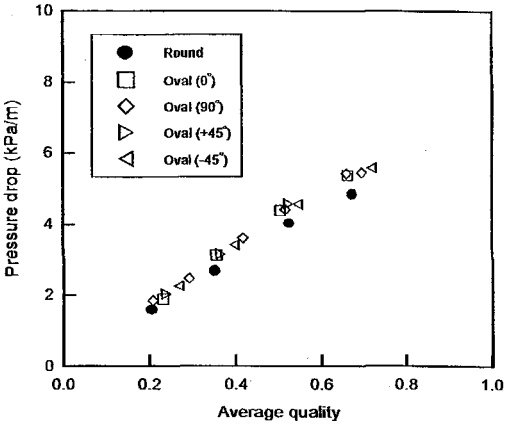

(b) Mass flow rate: 60 kg/h

Figure 9. Local pressure drops

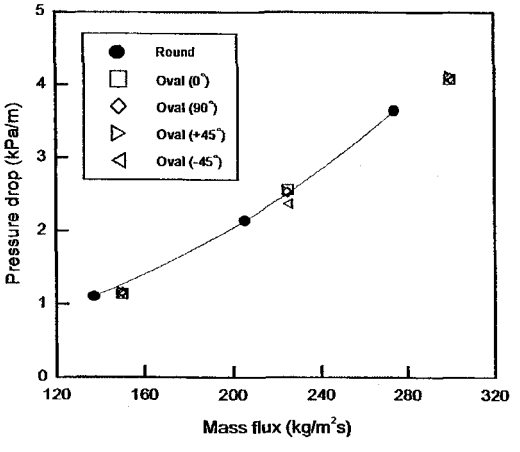

Figure 10. Average pressure drops with variation of mass flux

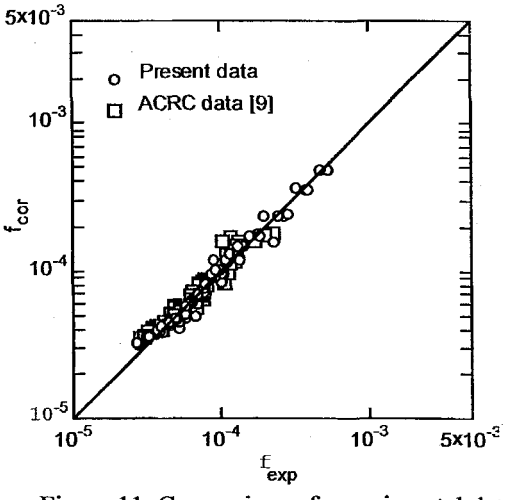

Figure 11. Comparison of experimental data and friction factor correlation